

Electrical properties of non-stoichiometric $\text{SmBa}_{0.5}\text{Sr}_{0.48}(\text{Co}_{1-x}\text{Fe}_x)_{2.05}\text{O}_{5+d}$ ($x = 0, 0.3, 0.5, 0.7$) layered perovskite cathodes for
SOFC

Jeong Yun Park^a, Yu Taek Hong^a, Yu Ri Lim^a, Bohyun Ryu^b, Harald Schlegl^c

, Jung Hyun Kim^{a,*}

^a Department of Advanced Materials Science and Engineering, Hanbat National University,
125, Dongseo-Daero, Yuseong-Gu, Daejeon, 34158, Republic of Korea

^b Fuel Cell Innovations (FCI) Co., Ltd. 41-7, Techno 11-ro, Yuseong-gu, Daejeon, Republic
of Korea

^c Physics Department, Lancaster University, Bailrigg, Lancaster, LA1 4YB, United Kingdom

Corresponding author: *

Jung Hyun Kim: jhkim2011@hanbat.ac.kr, jhkim1870@gmail.com,

Tel: +82-42-821-1239, Fax: +82-42-821-1592,

Department of Advanced Materials Science and Engineering, Hanbat National University, 125,
Dongseo-Daero, Yuseong-Gu, Daejeon, 34158, Republic of Korea

Abstract

In this study, the electrical properties of $\text{SmBa}_{0.5}\text{Sr}_{0.48}(\text{Co}_{1-x}\text{Fe}_x)_{2.05}\text{O}_{5+d}$ ($x = 0, 0.3, 0.5, 0.7$) (SBSCF) were analyzed under different oxygen partial pressures to find suitable candidates for cathodes for solid oxide fuel cells. Characteristic for these cathode materials are layered perovskite structures with a B-site excess non-stoichiometric composition.

The XRD analysis confirmed that all investigated SBSCF compositions with Co substitution exhibit a single-phase layered perovskite structure. Additionally, the XRD peaks exhibited shifts, separation, and merging depending on the Fe substitution amount.

SBSCF showed a behavior of decreasing electrical conductivity with increasing Fe substitution. The change in electrical conductivity was observed as the atmosphere was repeatedly varied between air and nitrogen environments, leading to a variation between high and low oxygen partial pressure. SBSCF exhibited higher electrical conductivity in an air atmosphere compared to a nitrogen atmosphere. Moreover, as the Fe substitution amount increased, the difference in electrical conductivity between the oxygen and nitrogen atmospheres became more pronounced. By repeatedly alternating between oxygen and nitrogen atmospheres and analyzing the electrical conductivity, it was confirmed that the SBSCF cathodes in this experiment demonstrated that after a heating and cooling process in a nitrogen atmosphere, the electrical conductivity recovers above 300 °C in air atmosphere, regardless of the amount of Fe substitution.

These results indicate that the SBSCF cathode exhibits reversible electrical conductivity behavior, meaning no or very little conductivity loss occurs under typical SOFC cathode conditions, even after changes in oxygen pressure and temperature. Consequently, the SBSCF oxide system demonstrates stable electrical conductivity properties.

Keywords: Solid oxide fuel cell (SOFC), Layered perovskite, Cathode, Electrical conductivity, Reversible electrical conductivity behavior

Highlight

- A layered perovskite with a non-stoichiometric composition, adjusted by varying the amount of Fe substitution, was selected.
- As the amount of Fe substitution increased, the electrical conductivity decreased.
- $\text{SmBa}_{0.5}\text{Sr}_{0.48}(\text{Co}_{0.3}\text{Fe}_{0.7})_{2.05}\text{O}_{5+d}$, which has the highest amount of Fe substitution, exhibited the smallest difference in electrical conductivity under various applied current.
- The SBSCF oxide system with a B-site excess composition of 2.05 exhibited stable “Reversible electrical conductivity” characteristics under varying oxygen partial pressure and thermal cycle conditions.

1. Introduction

In Solid Oxide Fuel Cells (SOFC), the oxygen reduction reaction (ORR) at the cathode is known to be slower compared to the oxidation reaction at the anode during electrochemical processes within the single cell [1]. Therefore, the development of cathodes with faster ORR kinetics is crucial for the enhancement of the SOFC performance. Additionally, SOFCs operate under varying oxygen partial pressures depending on temperature changes. Since oxygen partial pressure is closely related to the ORR at the cathode, understanding the electrical properties of the cathode under different oxygen partial pressure conditions is essential.

Layered perovskite oxides with mixed ionic and electronic conductivity (MIECs) have attracted significant attention as cathodes for solid oxide fuel cells [1-3]. Layered perovskites have the chemical formula $AA'B_2O_{5+\delta}$, where rare earth elements occupy the A-site, alkaline earth elements occupy the A'-site, and transition metals are located at the B-site. Additionally, the layered perovskite structure consists of alternating $[BO_2]$ - $[AO]$ - $[BO_2]$ - $[A'O]$ layers along the c-axis. This arrangement reduces the oxygen bonding strength in the $[AO]$ layer, providing a well-ordered ionic transport pathway that facilitates the diffusion of reactive oxygen ions. Among the layered perovskites, $LnBaCo_2O_{5+\delta}$ (Ln =rare earth metal) offers advantages such as high oxygen diffusion and surface exchange rates, flexible control of oxygen content and excellent ionic and electronic conductivity. Therefore, it is being investigated as a cathode material for solid oxide fuel cells [2, 4-7]. Layered perovskite structures based on Co oxides exhibit various oxidation states, including Co^{2+} , Co^{3+} , and Co^{4+} . In particular, the Co^{4+} oxidation state can maintain a large number of oxygen ion vacancies, which contributes to enhanced electrochemical performance. However, Co-based oxides exhibit a high coefficient of thermal expansion due to the transition of Co^{3+} ions from low-spin to high-spin states, as well as

chemical reactions with electrolyte materials. This leads to poor long-term operational stability and reduced cathode performance [8-10].

According to previous research conducted by our research group, the non-stoichiometric $\text{SmBa}_{0.5-x}\text{Sr}_{0.5-y}\text{Co}_z\text{O}_{5+d}$ ($x, y= 0.01 \sim 0.05, z= 1.9 \sim 2.1$, hereafter referred to as SBSCO) cathode exhibited the following electrical conductivity properties [11,12].

(1) It exhibited metallic behavior, with electrical conductivity decreasing as temperature increased under oxygen atmosphere generally and under nitrogen atmosphere during the heat up steps of a thermal cycling process. This behavior changed to semiconductor behavior during cooling under a nitrogen atmosphere.

(2) Electrical conductivity was measured at applied current levels of 0.1 A, 0.5 A, and 1.0 A. The highest electrical conductivity was observed at the lowest applied current of 0.1 A.

(3) $\text{SmBa}_{0.5}\text{Sr}_{0.48}\text{Co}_{2.05}\text{O}_{5+d}$ (SBSCO-0.5/0.48/2.05), an SBSCO composite with reduced Sr substitution at the perovskite A-site and excess Co substitution at the perovskite B-site, exhibited the highest electrical conductivity among all non-stoichiometric SBSCO compositions. TGA and XPS analyses revealed that upon heating of the composites above 300 °C, SBSCO-0.5/0.48/2.05 experienced the least reduction in oxygen content, leading to the formation of a large amount of oxygen vacancies. The analyses also indicated the highest level of Co^{3+} and Co^{4+} coexistence amongst all studied SBSCO compositions. Excessive Co substitution increases the concentration of oxygen vacancies, which can disrupt Co-O-Co bonds and limit charge carrier mobility. However, in the case of SBSCO-0.5/0.48/2.05, properly formed oxygen vacancies preserve the Co-O-Co bonds, enhancing charge carrier mobility and providing excellent electrical properties. Therefore, SBSCO-0.5/0.48/2.05 is considered the most suitable composition for achieving high electrical conductivity [11,12].

To maintain the excellent electrochemical performance of Co while minimizing associated issues, many researchers have investigated cathodes with Fe substitution. Fe substitution in Co-based cathodes has been reported to decrease the coefficient of thermal expansion, while also increasing catalytic activity and thermal stability [13]. According to Lim, C., et al., Fe substitution in the $\text{PrBa}_{0.8}\text{Ca}_{0.2}\text{Co}_2\text{O}_{5+\delta}$ cathode results in high cell performance of 1.89 W/cm^2 at $600 \text{ }^\circ\text{C}$, along with low thermal expansion coefficient and stable long-term performance [14]. Joo, S., et al. reported that Fe-substituted $\text{YBa}_{0.5}\text{Sr}_{0.5}\text{Co}_{1.75}\text{Fe}_{0.25}\text{O}_{5+\delta}$ cathode exhibited stable structural properties and reduced thermal expansion coefficient at operating temperature [15].

Therefore, research on improving the performance of Co-based cathodes through Fe substitution has primarily focused on stoichiometric compositions. Stability of cathode performance in atmospheres of varying degrees of oxygen partial pressure is important. The key factor determining cathode performance is the ORR reaction activity, which is influenced by a number of factors like catalytic activity, microstructure and very importantly electrical conductivity of the cathode material. For this reason, studies have analyzed the effect of thermal and oxygen partial pressure cycling on electrical conductivity by measuring the conductivity of cathode materials under specific oxygen partial pressures.

In this study, the focus was on investigating the effect of varying Fe B-site substitution on the electrical conductivity of $\text{SmBa}_{0.5}\text{Sr}_{0.48}(\text{Co}_{1-x}\text{Fe}_x)_{2.05}\text{O}_{5+d}$ ($x = 0, 0.3, 0.5, 0.7$) cathodes, a general composition which exhibits the highest electrical conductivity among the B-site excess non-stoichiometric layered perovskites.

In summary, the electrical conductivity was measured as a function of the Co/Fe ratio by varying the amount of Fe substitution. The conditions for the electrical conductivity measurements were as follows: heating and cooling process within the temperature range of

50 °C to 900 °C, with applied current of 0.1 A, 0.5 A and 1.0 A. Additionally, electrical conductivity and thermal cycle stability under continuous fluctuations in oxygen partial pressure were investigated by alternating between oxygen and nitrogen atmospheres.

2. Experimental

2.1 Phase synthesis

The layered perovskite structure $\text{SmBa}_{0.5}\text{Sr}_{0.48}(\text{Co}_{1-x}\text{Fe}_x)_{2.05}\text{O}_{5+d}$ ($x = 0, 0.3, 0.5, 0.7, 1.0$) cathodes were synthesized using a solid-state reaction method. The starting materials used were Sm_2O_3 (Alfa Aesar, 99.9%), BaCO_3 (Samchun, 99.0%), SrCO_3 (Aldrich, 99.9%), Co_3O_4 (Alfa Aesar, 99.7%) and Fe_3O_4 (Kojundo, 99.0%) powders, which were accurately weighed according to the target composition. The weighed powder was uniformly mixed in an agate mortar, and a small amount of ethanol was added to prevent powder loss. The mixed powder was dried in an oven at 78 °C for 24 hours and primary calcined at 1000 °C for 6 hours. After the primary calcination, the powders were ball-milled for 24 hours at 120 rpm using acetone as a solvent to ensure uniform grinding. The acetone was evaporated by drying the mixture in an oven at 78 °C. The dried, primary calcined powder was subject to a second grinding step, again using an agate mortar followed by a secondary calcination at 1100 °C for 8 hours to form a single phase. Finally, the powders were ground for a third time to finally obtain five SBSCF cathode powders with different Co to Fe ratios. The abbreviations used for these different cathode compositions based on the amount of their Fe substitution are summarized in Table 1.

2.2 Phase analysis

The phase formation and properties of the crystal structure of the different cathode powders synthesized by the solid state reaction were analyzed using X-ray diffraction (Rigaku, Japan, SmartLab). The analysis used Cu K α radiation, set at 45 kV and 200 mA, with a 2θ range from 0° to 90°. The XRD results were analyzed using the MDI JADE 6 software.

2.3 Electrical conductivity analysis

To measure the electrical conductivity using the 4-probe method, powders of each composition were compacted at a pressure of 1.8×10^3 kg/m 2 . The compacted powders were then sintered in an air atmosphere at 1100 °C for 3 hours to produce dense bar-type samples.

The electrical conductivity of the prepared bar-type samples was measured using the DC 4-probe method. The samples were connected to a Keithley 2400 source meter using Pt wires for the measurements. Detailed information about the measurement equipment can be found in papers previously published by our research group [12, 16].

In contrast to previously reported studies parameters like the partial pressure of oxygen, measurement temperature and applied current were simultaneously varied during the measurement of the electrical conductivity. The detailed measurement conditions are summarized in Table 2.

As shown in Table 2, the heating process (increasing the temperature from 50 °C to 900 °C) and the cooling process (decreasing the temperature from 900 °C to 50 °C) were carried out in 50°C intervals. To analyze the variation in electrical conductivity with repeated changes in oxygen partial pressure, a series of 6 cycles was conducted to measure the electrical conductivity. Cycles 1, 3, and 5 were conducted in an air atmosphere with applied currents of 0.1 A, 0.5 A, and 1.0 A for each temperature during both the heating and cooling processes.

Cycles 2, 4, and 6 were carried out in a nitrogen atmosphere, with the same heating and cooling temperature and applied current conditions as in the air atmosphere. The nitrogen atmosphere was established using 99.95% pure nitrogen gas at a flow rate of 1 cc/min. Before the measurements, the gas was introduced and maintained for 30 minutes to purge gases formerly present and to ensure the formation of a sufficiently stable nitrogen atmosphere. In other words, the electrical conductivity was measured in alternating air and nitrogen atmospheres to confirm the stability of the cathode's electrical properties under changing partial pressure of oxygen conditions.

3. Result and discussion

3.1 XRD analysis

The results of the XRD analysis, used to determine the phase formation of the $\text{SmBa}_{0.5}\text{Sr}_{0.48}(\text{Co}_{1-x}\text{Fe}_x)_{2.05}\text{O}_{5+d}$ ($x=0, 0.3, 0.5, 0.7, 1.0$) oxide system, are summarized in Figure 1.

The XRD patterns with distinctive peaks observed at 32.9° , 40.5° , 46.8° , and 58.5° indicate that the SBSCF 2.05-0, 0.3, 0.5, and 0.7 cathodes synthesized via solid-state reaction exhibit a layered perovskite structure. In contrast, SBSCF 2.05-1.0 was found to be non-single phase due to the formation of secondary phases, such as Sm_2O_3 and SrFe_2O_6 . The cathode composition SBSCF 2.05-1.0 was therefore excluded from the electrical conductivity analysis. Thus, in this oxide system, the Co to Fe ratio ($1-x/x$) must be at least 0.429 to obtain a single-phase structure.

XRD analysis indicated that the main peak shifted to the left as the amount of Fe substitution increased, emerging at a 2θ value of more than 33° for SBSCF 2.05-0 gradually decreasing to

a 2θ value of less than 32.5° for SBSCF 2.05-0.7. This peak shift is attributed to the difference in ionic radii between Fe^{3+} ($r=0.645\text{\AA}$) and Co^{3+} ($r=0.61\text{\AA}$). As the amount of Fe substitution increases, the lattice parameter and unit cell volume expand due to the larger ionic radius of Fe^{3+} compared to Co^{3+} [17]. The formation of secondary phases in SBSCF 2.05-1.0 is likely due to the instability of the perovskite lattice, which is too small to accommodate the large Fe^{3+} ions, ultimately leading to the formation of these secondary phases.

SBSCF 2.05-0.3 exhibits XRD patterns with two peaks corresponding to (110) and (102) around 33° , while SBSCF 2.05-0.5 and SBSCF 2.05-0.7 show only a single (110) peak. This is consistent with findings in previous literature and indicates that the crystal structure of SBSCF cathodes transitions from a tetragonal symmetry to a cubic symmetry as the amount of Fe substitution increases [18].

Thus, in the SBSCF oxide system, single-phase structures can be achieved even in excess non-stoichiometric compositions where the sum of Co and Fe at the B-site of the perovskite is 0.05 greater than the typical stoichiometric value, as long as the x value is 0.7 or less.

3.2 Electrical conductivity as a function of Fe substitution

Figure 2 summarizes the results of electrical conductivity as a function of Fe substitution amount, with a current of 0.1 A applied.

Fe-substituted SBSCF 2.05-0.3, 0.5, and 0.7 exhibited an increase in electrical conductivity from room temperature, reaching a maximum around 300°C . Above this temperature the electrical conductivity decreases, indicating a metal-insulator transition (MIT) behavior.

In addition, SBSCF 2.05-0.3, 0.5, and 0.7 showed higher electrical conductivity values measured in an air atmosphere (triangle symbols) compared to those in a nitrogen atmosphere (circle symbols), indicating the presence of p-type conductors, where electron holes serve as charge carriers. This electrical conductivity behavior can be explained by the p-type small polaron hopping mechanism. In the low temperature region below 300 °C, where the highest electrical conductivity values are observed, the increase in conductivity is attributed to the hopping of charge carriers through the $(\text{Co}, \text{Fe})^{3+}\text{-O}^{2-}\text{-(Co}, \text{Fe})^{4+}$ sites. However, in the high-temperature region above 300 °C, thermal reduction of $(\text{Co}, \text{Fe})^{4+}$ occurs with increasing temperature, leading to the formation of a large number of oxygen vacancies. This interferes with the mobility of electron holes, reducing electrical conductivity at high temperatures [19-21]. Therefore, it can be concluded that the electrical conductivity properties of the SBSCF 2.05 oxide system are attributed to electron hole hopping in the low temperature region and the limitation of charge carrier mobility due to oxygen vacancy formation in the high temperature region.

It is interesting to observe that this behavior with a maximum conductivity at around 300 °C is clearly a function of the amount of Fe substitution x . In the composition SBSCF 2.05-0, a composition without Fe substitution, there is no conductivity local maximum at all, the conductivity is very high at low temperatures and keeps decreasing with increasing temperature in a way resembling the conductivity behavior of metals. The conductivity maximum is barely visible for the composition SBSCF 2.05-0.3, while in the composition with the highest amount of Fe substitution, SBSCF 2.05-0.7, the conductivity maximum at around 300 °C is very pronounced and clearly visible. One possible explanation could be that the polaron hopping mechanism described above is characteristic for the presence of plenty of Fe at the B-site of SBSCF.

Comparing the electrical conductivity at 700 °C in air atmosphere, realistic working conditions for an IT-SOFC cathode, SBSCF 2.05-0 exhibits the highest electrical conductivity at 256.3 S/cm. SBSCF 2.05-0.3 shows a conductivity of 188.2 S/cm at the same temperature during heating process, while SBSCF 2.05-0.5 exhibits 58.9 S/cm, and SBSCF 2.05-0.7 shows 23.6 S/cm. This indicates a trend where electrical conductivity decreases as the amount of substituted Fe increases. These electrical conductivity values exhibited a behavior similar to that of LSCF, a widely studied SOFC cathode material. Lee et al. reported that in $\text{LaSr}_3\text{Fe}_{3-y}\text{Co}_y\text{O}_{10-\delta}$ ($0 \leq y \leq 1.5$), electrical conductivity increases as the Co substitution amount increases, achieving around 200 S/cm at 700 °C for $\text{LaSr}_3\text{Fe}_{1.5}\text{Co}_{1.5}\text{O}_{10-\delta}$ and around 160 S/cm at 700 °C for $\text{LaSr}_3\text{Fe}_2\text{CoO}_{10-\delta}$, quite similar conductivity values to SBSCF. Notably, comparing the most Co-rich examples of LSCF and SBSCF, SBSCF 2.05-0 and SBSCF 2.05-0.3 exhibited slightly higher electrical conductivity values (256.3 S/cm and 188.2 S/cm) than $\text{LaSr}_3\text{Fe}_{1.5}\text{Co}_{1.5}\text{O}_{10-\delta}$ and $\text{LaSr}_3\text{Fe}_2\text{CoO}_{10-\delta}$ (~200 S/cm and ~160 S/cm), respectively [22]. This behavior of the SBSCF 2.05 oxide system is consistent with the tendency observed in stoichiometric compositions, where electrical conductivity decreases with increasing Fe substitution. To explain this tendency, it is worth mentioning that Fe^{3+} has a larger ionic radius compared to Co^{3+} , so when Fe^{3+} is substituted for Co^{3+} at the B-site, the amount of overlap between the $(\text{Co/Fe})^{3+/4+}$: 3d orbital and the O^{2-} :2p orbital decreases, leading to an increase in the charge transfer gap. Additionally, the covalency of the bonds between (Co, Fe) and oxygen decreases, reducing the mobility of charge carriers and, consequently, electrical conductivity [10, 18, 22]. This mechanism apparently also applies to non-stoichiometric compositions with B-site excess, like the SBSCF 2.05 compositions studied in this paper.

3.3 Electrical conductivity differences with applied current

Figure 3 compares the difference in electrical conductivity at 600 °C under applied currents of 0.1 A, 0.5 A, and 1.0 A. Figure 3 (a) shows the electrical conductivity measurement during the heating process of SBSCF 2.05-0 in an air atmosphere. The highest electrical conductivity observed was 335.2 S/cm with a 0.1 A applied current, followed by 265.0 S/cm at 0.5 A and 259.5 S/cm at 0.1 A. Thus, the electrical conductivity was found to be inversely proportional to the applied current. Figure 3 indicates that the electrical conductivity is highest at 0.1 A for all compositions of the SBSCF oxide system. This behavior can be explained by the fact that, as the applied current increases, the number of charge carriers moving through the same crystal lattice also increases. As a result, the transport paths of the charge carriers within the lattice become more obstructed, leading to the observed decrease in electrical conductivity for a higher current [23]. Therefore, the relationship between the applied current and electrical conductivity remained inversely proportional, regardless of changes in measurement conditions such as oxygen partial pressure and temperature.

On the other hand, the difference in electrical conductivity with varying applied current decreases as the amount of Fe substitution increases. The specific electrical conductivity values measured at 600 °C during heating process in an air atmosphere are summarized in Table 3.

For SBSCF 2.05-0 without Fe substitution, the electrical conductivity at an applied current of 0.1 A (335.2 S/cm) is approximately 1.3 times higher than the conductivity at 0.5 A (265.0 S/cm), as shown in Figure 3 (a) and Table 3. In contrast, for Fe-substituted SBSCF oxide system, the difference in electrical conductivity decreased when the same currents were applied: SBSCF 2.05-0.3 showed 109.7 S/cm at 0.5 A and 119.8 S/cm at 0.1 A (difference: 9.2%), SBSCF 2.05-0.5 showed 37.3 S/cm at 0.5 A and 38.3 S/cm at 0.1 A (difference: 2.7%), and SBSCF 2.05-0.7 showed 16.6 S/cm at 0.5 A and 17.0 S/cm at 0.1 A (difference: 2.4%). Specifically, for SBSCF 2.05-0.7, very similar electrical conductivity values were observed

over the whole range of applied currents. The reason for these similar conductivity values at 0.1 A and 0.5 A with increasing Fe substitution can be explained as follows.

First, the difference in electrical conductivity due to Fe substitution arises from the reduction in oxygen vacancies. The bond strength of Fe-O is stronger than that of Co-O, resulting in fewer oxygen ions dissociating from Fe compared to Co. Consequently, the number of oxygen ions leaving the lattice is relatively lower when bonded with Fe [24]. In other words, as the Fe substitution increases, oxygen loss becomes more limited, leading to decrease in the concentration of oxygen vacancies generated.

Second, the decrease in the electrical conductivity difference with increasing applied current is due to oxygen vacancies in the cathode hindering the movement of charge carriers at higher currents, leading to a reduction in conductivity. However, Fe substitution mitigates this decrease in conductivity by reducing the concentration of oxygen vacancies in the lattice, thereby making charge carrier transport more efficient. As a result, the concentration of oxygen vacancies decreases with increasing Fe substitution. The difference in conductivity with applied current is smallest in SBSCF 2.05-0.7, the composition with the highest level of Fe substitution [25, 26].

This behavior of the differences in electrical conductivity between 0.1 A and 0.5 A due to varying degrees of Fe substitution prove consistent across all other measurement conditions, including air and nitrogen atmospheres, as well as during both heating and cooling processes, as demonstrated in Figure 3. When measured during cooling in an air atmosphere, SBSCF 2.05-0 showed the largest difference in electrical conductivity, as seen in Figure 3 (b). Furthermore, as the amount of Fe substitution increases, the difference in electrical conductivity between 0.1 A and 0.5 A decreases significantly. This behavior is similar to the results observed during

heating in an air atmosphere, shown in Figure 3 (a). The same trend is also observed under a nitrogen atmosphere for both heating and cooling conditions, as illustrated in Figures 3 (c) and 3 (d). These results demonstrate that the differences in electrical conductivity values at different applied currents are not influenced by measurement conditions such as oxygen partial pressure or temperature cycle variations. This behavior is inherent to the SBSCF 2.05 oxide system. Therefore, the differences in electrical conductivity values when applying 0.1 A and 0.5 A currents are characteristics intrinsic to the SBSCF 2.05 oxide system. Increased Fe substitution leads to the formation of fewer oxygen vacancies, allowing charge carriers to move more freely. As a result, the difference in electrical conductivity with varying applied current is reduced.

3.4 Electrical conductivity with changing oxygen partial pressure

According to the electrical conductivity analysis in Section 3.2, the non-stoichiometric SBSCF 2.05 oxide system exhibits p-type conduction properties, with lower electrical conductivity as oxygen partial pressure decreases. A common method for analyzing electrical conductivity is to compare it under specific oxygen partial pressures. Studies have shown that a decrease in oxygen partial pressure reduces the concentration of holes, which are the charge carriers in p-type conductors, thereby decreasing electrical conductivity [27-29]. Therefore, understanding the electrical conductivity characteristics in relation to oxygen partial pressure is critical for elucidating the electrochemical mechanisms of cathodes.

To investigate the changes in electrical conductivity of the SBSCF 2.05 oxide system with variations in oxygen partial pressure and thermal cycling, the electrical conductivity was measured by alternating between air and nitrogen atmospheres from cycle 1 to cycle 6. During each cycle both a heating process from 50 °C to 900 °C and a cooling process from 900 °C to

50 °C were performed, conductivity measurements applying currents of 0.1 A, 0.5 A, and 1.0 A were carried out in intervals of 50 °C. The measurement conditions are shown in Table 2. Additionally, the values measured at 300 °C with a current of 0.1 A applied to each sample are summarized in Table 4. As shown in Figure 4 (a) and Table 4, SBSCF 2.05-0 exhibited metallic behavior in all cycles. In Cycle 1, measured in an air atmosphere, the electrical conductivity was 787.4 S/cm at 300 °C during the heating process and 790.3 S/cm during the cooling process. During the heating process in Cycle 2, measured in a nitrogen atmosphere, the electrical conductivity was 717.2 S/cm, lower than in Cycle 1. During the cooling process, the conductivity decreased significantly to 406.6 S/cm. However, when the air atmosphere was restored in Cycle 3, the electrical conductivity increased to 646.3 S/cm during the heating process and 714.7 S/cm during cooling, showing values similar to those in Cycle 1 at the same temperature. This same behavior was observed in Cycles 4, 5, and 6 as well. Therefore, the SBSCF 2.05-0 cathode demonstrates stable electrical conductivity in various oxygen partial pressure environments. Additionally, the compositions synthesized with only Co present at the perovskite B-site exhibited stability to thermal cycling.

The Fe-substituted SBSCF 2.05-0.3, SBSCF 2.05-0.5, and SBSCF 2.05-0.7 cathodes showed a different conductivity behavior to SBSCF in some ways. For once, instead of the metal like decrease of conductivity over the whole temperature range seen in SBSCF 2.05-0, the Fe containing composites show a local maximum of conductivity around 300 °C, a phenomenon described and explained by the polaron hopping mechanism in chapter 3.2. Secondly the decrease of conductivity values with a decrease of oxygen partial pressure is much more extreme in all Fe substituted compositions, especially at relatively low temperatures, reached during the cool down phase under nitrogen atmosphere.

For SBSCF 2.05-0.3 (Figure 4 (b)), the electrical conductivity during the heating process to 300 °C in an air atmosphere (Cycle 1) was 248.8 S/cm, while during the cooling process, it increased slightly to 262.0 S/cm. In Cycle 2, with a lower oxygen partial pressure, the electrical conductivity was 248.6 S/cm during heating but decreased to 112.6 S/cm during cooling. In Cycle 3, when the air atmosphere was reintroduced, the conductivity started at a value similar to the lowest observed during cooling in Cycle 2 and gradually increased, recovering to 191.4 S/cm at 300 °C. Similar behavior was observed in subsequent cycles.

In Figure 4 (c), which summarizes the electrical conductivity of SBSCF 2.05-0.5, a decline in electrical conductivity occurred in all cycles with nitrogen atmospheres during the cooling processes. During heating in Cycle 1, the electrical conductivity at 300 °C was 38.4 S/cm, while during the cooling process at the same temperature, it dropped slightly to 37.5 S/cm. In a nitrogen atmosphere during Cycle 2, the electrical conductivity was measured to be 32.4 S/cm during the heating process and 21.6 S/cm during the cooling process. As with previous results, a decrease in electrical conductivity was observed during cooling in the nitrogen atmospheres of Cycle 2 and Cycle 4. However, when the air atmosphere was reintroduced in Cycle 3 and Cycle 5, an increase in electrical conductivity was observed.

In Figure 4 (d), SBSCF 2.05-0.7, a composition with relatively high Fe substitution, exhibited the lowest electrical conductivity among all compositions. During the cooling process in a nitrogen atmosphere, both metal-insulator transition (MIT) behavior and semiconductor behavior were observed simultaneously. In Cycle 2 and Cycle 4, semiconductor behavior was predominant during the cooling process. However, the electrical conductivity results for Cycle 3 and Cycle 5 show that conductivity increased in the low-temperature range, recovering around 300 °C.

In Figure 4, by repeatedly alternating between air and nitrogen atmospheres, the electrical conductivity of the SBSCF 2.05 oxide system was analyzed in response to changes in oxygen partial pressure, revealing the following characteristics:

(1) For all compositions, measurements in a nitrogen atmosphere resulted in a rapid decrease in electrical conductivity, confirming that the SBSCF oxide system is a p-type conductor.

(2) The decrease in electrical conductivity observed during cooling in a nitrogen atmosphere in Cycle 2 and Cycle 4 recovered after returning to an air atmosphere and heating to temperatures near 300 °C, achieving values similar to those in Cycle 3 and Cycle 5.

(3) As the amount of Fe substitution increased, the electrical conductivity decreased even more significantly during the cooling process in a nitrogen atmosphere. For SBSCF 2.05-0.7, with the highest Fe substitution, semiconductor behavior was observed during the cooling process in Cycle 2 and Cycle 4. Despite the low electrical conductivity in the nitrogen atmosphere, subsequent measurements in an air atmosphere showed that the conductivity recovered to values previously seen in air around 300 °C.

The mechanism of such “Reversible Electrical Conductivity Behavior” can be interpreted using the p-type small polaron hopping mechanism described in Section 3.2. The electrical conductivity of SBSCF decreases when cooling in a nitrogen atmosphere during Cycle 2, and when the air atmosphere is reintroduced in Cycle 3, the electrical conductivity fully recovers to the same level as in Cycle 1. In general, an air atmosphere has a high oxygen partial pressure, leading to the oxidation of Co^{3+} and Fe^{3+} into Co^{4+} and Fe^{4+} . This oxidation increases the concentration of electron holes, which act as charge carriers, thereby resulting in relatively high electrical conductivity. However, in a nitrogen atmosphere, oxygen ions are removed, increasing the oxygen vacancy concentration and causing the reduction of Co^{4+} and Fe^{4+} back

to Co^{3+} and Fe^{3+} . Consequently, the decrease in electron hole concentration leads to a reduction in electrical conductivity. In particular, during the cooling process in a nitrogen atmosphere, in addition to the lower concentration of electron holes, their mobility is further hindered by oxygen vacancies, resulting in even lower electrical conductivity. However, when the oxygen atmosphere is reintroduced, the previously removed oxygen is reinserted into the electrode, restoring the electron hole concentration and consequently recovering the electrical conductivity. Furthermore, since the recovery of electrical conductivity occurs around 300 °C, it is inferred that the reinsertion of oxygen into the electrode proceeds gradually at temperatures below 300 °C and is completed at 300 °C [30].

This mechanism indicates that the SBSCF 2.05 oxide system with a B-site excess non-stoichiometric composition exhibits stable and recoverable electrical conductivity properties, even in environments with fluctuating oxygen partial pressures. Consequently, it can be concluded that the system demonstrates reversible electrical conductivity behavior.

4. Conclusion

In this study, the electrical properties of the $\text{SmBa}_{0.5}\text{Sr}_{0.48}(\text{Co}_{1-x}\text{Fe}_x)_{2.05}\text{O}_{5+d}$ ($x = 0, 0.3, 0.5, 0.7$) oxide system, a non-stoichiometric layered perovskite structure with excess Co and Fe substituted at the B-site, were analyzed based on the amount of Fe substitution, applied current, and variations in oxygen partial pressure.

The SBSCF 2.05 oxide system, prepared by solid-state reaction, exhibits a single-phase, layered perovskite structure. The range of Fe substitution that allows for a single-phase structure is from 0 to 0.7 for x .

Comparing the electrical conductivity of the SBSCF 2.05 oxide system with different Fe substitutions, all samples except SBSCF 2.05-0 exhibited metal-insulator transition (MIT) behavior. Furthermore, due to the reduced covalency between (Co, Fe) and oxygen caused by the larger ionic radius of Fe, electrical conductivity decreased as the amount of Fe substitution increased. When electrical conductivity was measured with applied currents of 0.1 A, 0.5 A, and 1.0 A, SBSCF 2.05-0.7 exhibited the smallest difference between the conductivity measured at higher currents and the conductivity measured at lower currents. During electrical conductivity measurements under varying oxygen partial pressures, all compositions showed a decrease in conductivity in the nitrogen atmosphere of Cycle 2. However, after returning to the oxygen atmosphere in Cycle 3, the electrical conductivity recovered to levels similar to those in Cycle 1 at 300 °C. Thus, all compositions demonstrated adequate electrical conductivity at operating temperatures, confirming that the excess non-stoichiometric composition of $\text{SmBa}_{0.5}\text{Sr}_{0.48}(\text{Co}_{1-x}\text{Fe}_x)_{2.05}\text{O}_{5+d}$ is suitable for use as cathode in solid oxide fuel cells.

Acknowledgements

This work was supported by the Human Resources Development of the Korea Institute of Energy Technology Evaluation and Planning (KETEP) grant funded by the Korea government (No. RS-2024-00394769) and Basic Science Research Program through the National Research Foundation of Korea (NRF) funded by the Ministry of Education (No. RS-2024-00464203).

Declaration of competing interest

The authors declare that they have no known competing financial interests or personal relationships that could have appeared to influence the work reported in this paper.

References

- [1] O. Yamamoto, Solid oxide fuel cells: fundamental aspects and prospects, *Electrochim. Acta*. 45 (2000) 2423–2435. [https://doi.org/10.1016/S0013-4686\(00\)00330-3](https://doi.org/10.1016/S0013-4686(00)00330-3).
- [2] A.K. Azad, J.H. Kim, J.T.S. Irvine, Structure–property relationship in layered perovskite cathode $\text{LnBa}_{0.5}\text{Sr}_{0.5}\text{Co}_2\text{O}_{5+\delta}$ (Ln= Pr, Nd) for solid oxide fuel cells, *J. Power Sources*. 196 (2011). 7333–7337. <https://doi.org/10.1016/j.jpowsour.2011.02.063>.
- [3] J.M. Im, K.E. Song, H. Schlegl, H. Kang, W. Choi, S.-W. Baek, J.-Y. Park, H.-S. Kim, J.H. Kim, Generation of nanoflowers and nanoneedles on Co-based layered perovskite of IT-SOFC cathode affecting electrical conductivities, *Int. J. Hydrogen Energy*. 48 (2023) 35229–35239. <https://doi.org/10.1016/j.ijhydene.2023.05.327>.
- [4] X. Kong, G. Liu, Z. Yi, X. Ding, $\text{NdBaCu}_2\text{O}_{5+\delta}$ and $\text{NdBa}_{0.5}\text{Sr}_{0.5}\text{Cu}_2\text{O}_{5+\delta}$ layered perovskite oxides as cathode materials for IT-SOFCs, *Int. J. Hydrogen Energy*. 40 (2015) 16477–16483. <https://doi.org/10.1016/j.ijhydene.2015.09.006>.
- [5] S. Yoo, S. Choi, J. Kim, J. Shin, G. Kim, Investigation of layered perovskite type $\text{NdBa}_{1-x}\text{Sr}_x\text{Co}_2\text{O}_{5+\delta}$ ($x = 0, 0.25, 0.5, 0.75,$ and 1.0) cathodes for intermediate-temperature solid oxide fuel cells, *Electrochim. Acta*. 100 (2013) 44–50. <http://dx.doi.org/10.1016/j.electacta.2013.03.041>.
- [6] X. Bao, X. Su, S. Wang, B. Pan, L. Wang, L. Zhang, Z. Song, W. Long, C. Li, Effects of Bi-doping on structure and properties of $\text{YBaCo}_2\text{O}_{5+\delta}$ layered perovskite cathode for intermediate-temperature solid oxide fuel cells, *J. Alloys Compd*. 965 (2023) 171391. <https://doi.org/10.1016/j.jallcom.2023.171391>.
- [7] S.L. Pang, X.N. Jiang, X.N. Li, H.X. Xu, L. Jiang, Q.L. Xu, Y.C. Shi, Q.Y. Zhang, Structure and properties of layered-perovskite $\text{LaBa}_{1-x}\text{Co}_2\text{O}_{5+\delta}$ ($x = 0-0.15$) as intermediate-temperature

- cathode material, *J. Power Sources.* 240 (2013) 54–59.
<https://doi.org/10.1016/j.jpowsour.2013.04.005>.
- [8] C. Lu, B. Niu, W. Yi, Y. Ji, B. Xu, Efficient symmetrical electrodes of $\text{PrBaFe}_{2-x}\text{Co}_x\text{O}_{5+\delta}$ ($x = 0, 0.2, 0.4$) for solid oxide fuel cells and solid oxide electrolysis cells, *Electrochim. Acta.* 358 (2020) 136916. <https://doi.org/10.1016/j.electacta.2020.136916>.
- [9] J. Bai, D. Zhou, L. Niu, R. Chen, X. Zhu, N. Wang, Q. Liang, W. Yan, Sc-doped Co-based perovskites as IT-SOFC cathode with high oxygen reduction reaction and CO_2 tolerance, *Solid State Ionics.* 402 (2023) 116377. <https://doi.org/10.1016/j.ssi.2023.116377>.
- [10] K.T. Lee, A. Manthiram, Effect of cation doping on the physical properties and electrochemical performance of $\text{Nd}_{0.6}\text{Sr}_{0.4}\text{Co}_{0.8}\text{M}_{0.2}\text{O}_{3-\delta}$ ($\text{M} = \text{Ti, Cr, Mn, Fe, Co, and Cu}$) cathodes, *Solid State Ionics.* 178 (2007) 995–1000. <https://doi.org/10.1016/j.ssi.2007.04.010>.
- [11] K.E. Song, H. Schlegl, H. Kang, W. Choi, J.H. Kim, Electrochemical characteristic of non-stoichiometric $\text{SmBa}_{0.45}\text{Sr}_{0.5}\text{Co}_2\text{O}_{5+\delta}$ layered perovskite oxide system for IT-SOFC cathode, *Int. J. Hydrogen Energy.* 48 (2023) 17664–17676. <https://doi.org/10.1016/j.ijhydene.2023.01.255>.
- [12] J.M. Im, H. Schlegl, J.-Y. Park, S.-W. Baek, J.H. Kim, Electrochemical properties of B-site non-stoichiometric layered perovskite $\text{SmBa}_{0.5}\text{Sr}_{0.5}\text{Co}_x\text{O}_{5+\delta}$ ($x = 1.9\text{--}2.1$) cathodes for IT-SOFC, *Ceram. Int.* 50 (2024) 24565–24575. <https://doi.org/10.1016/j.ceramint.2024.04.192>.
- [13] T. Ghorbani-Moghadam, A. Kompany, M. Golmohammad, The comparative study of doping Cu and Fe on the cathodic properties of $\text{La}_{0.7}\text{Sr}_{1.3}\text{CoO}_4$ layered perovskite compound: To be used in IT-SOFC, *J. Alloys Compd.* 926 (2022) 166928. <https://doi.org/10.1016/j.jallcom.2022.166928>.
- [14] C. Lim, S. Sengodan, D. Jeong, J. Shin, G. Kim, Investigation of the Fe doping effect on the B-site of the layered perovskite $\text{PrBa}_{0.8}\text{Ca}_{0.2}\text{Co}_2\text{O}_{5+\delta}$ for a promising cathode material of

- the intermediate-temperature solid oxide fuel cells, *Int. J. Hydrogen Energy*. 44 (2019) 1088–1095. <https://doi.org/10.1016/j.ijhydene.2018.10.182>.
- [15] S. Joo, J. Kim, J. Shin, T.-H. Lim, G. Kim, Investigation of a layered perovskite for IT-SOFC cathodes: B-site Fe-doped $\text{YBa}_{0.5}\text{Sr}_{0.5}\text{Co}_{2-x}\text{Fe}_x\text{O}_{5+\delta}$, *J. Electrochem. Soc.* 163 (2016) F1489. <http://dx.doi.org/10.1149/2.0371614jes>.
- [16] K.E. Song, H. Schlegl, C.G. Kim, K.S. Baek, Y.R. Lim, J.H. Nam, H.S. Kim, J.H. Kim, Electrical conductivity properties of porous $\text{SmBaCo}_2\text{O}_{5+\delta}$ and $\text{SmBa}_{0.5}\text{Sr}_{0.5}\text{Co}_2\text{O}_{5+\delta}$ layered perovskite oxide systems for solid oxide fuel cell, *Ceram. Int.* 48 (2022) 28649–28658. <https://doi.org/10.1016/j.ceramint.2022.06.179>.
- [17] A. Jun, S. Yoo, Y.-W. Ju, J. Hyodo, S. Choi, H.Y. Jeong, J. Shin, T. Ishihara, T.-H. Lim, G. Kim, Correlation between fast oxygen kinetics and enhanced performance in Fe doped layered perovskite cathodes for solid oxide fuel cells, *J. Mater. Chem. A* 3 (2015) 15082–15090. <https://doi.org/10.1039/C5TA02158H>.
- [18] J. Zou, J. Park, B. Kwak, H. Yoon, J. Chung, Effect of Fe doping on $\text{PrBaCo}_2\text{O}_{5+\delta}$ as cathode for intermediate-temperature solid oxide fuel cells, *Solid State Ionics*. 206 (2012) 112–119. <https://doi.org/10.1016/j.ssi.2011.10.025>.
- [19] Z. Li, B. Wei, Z. Lü, X. Huang, W. Su, Structure, electrical and thermal properties of $(\text{Ba}_{0.5}\text{Sr}_{0.5})_{1-x}\text{Gd}_x\text{Co}_{0.8}\text{Fe}_{0.2}\text{O}_{3-\delta}$ perovskite as a solid-oxide fuel cell cathode, *Solid State Ionics*. 207 (2012) 38–43. <https://doi.org/10.1016/j.ssi.2011.11.024>.
- [20] H. Patra, S.K. Rout, S.K. Pratihari, S. Bhattacharya, Thermal, electrical and electrochemical characteristics of $\text{Ba}_{1-x}\text{Sr}_x\text{Co}_{0.8}\text{Fe}_{0.2}\text{O}_{3-\delta}$ cathode material for intermediate temperature solid oxide fuel cells, *Int. J. Hydrogen Energy*. 36 (2011) 11904–11913. <https://doi.org/10.1016/j.ijhydene.2011.06.021>.

- [21] F. Jin, J. Li, Y. Wang, X. Chu, M. Xu, Y. Zhai, Y. Zhang, W. Fang, P. Zou, T. He, Evaluation of Fe and Mn co-doped layered perovskite $\text{PrBaCo}_{2/3}\text{Fe}_{2/3}\text{Mn}_{1/2}\text{O}_{5+\delta}$ as a novel cathode for intermediate-temperature solid-oxide fuel cell, *Ceram. Int.* 44 (2018) 22489–22496. <https://doi.org/10.1016/j.ceramint.2018.09.018>.
- [22] K.T. Lee, A. Manthiram, $\text{LaSr}_3\text{Fe}_{3-y}\text{Co}_y\text{O}_{10-\delta}$ ($0 \leq y \leq 1.5$) intergrowth oxide cathodes for intermediate temperature solid oxide fuel cells, *Chem. Mater.* 18 (2006) 1621–1626. <https://doi.org/10.1021/cm052645+>.
- [23] K.S. Baek, S.-W. Baek, H. Kang, W. Choi, J.-Y. Park, S. Saxin, S.K. Lee, J.H. Kim, Electrical conductivity characteristics of Sr substituted layered perovskite cathode ($\text{SmBa}_{0.5}\text{Sr}_{0.5}\text{Co}_2\text{O}_{5+\delta}$) for intermediate temperature-operating solid oxide fuel cell, *Ceram. Int.* 48 (2022) 15770–15779. <https://doi.org/10.1016/j.ceramint.2022.02.114>.
- [24] X. Pan, Z. Wang, B. He, S. Wang, X. Wu, C. Xia, Effect of Co doping on the electrochemical properties of $\text{Sr}_2\text{Fe}_{1.5}\text{Mo}_{0.5}\text{O}_6$ electrode for solid oxide fuel cell, *Int. J. Hydrogen Energy.* 38 (2013) 4108–4115. <https://doi.org/10.1016/j.ijhydene.2013.01.121>.
- [25] F. Chen, D. Zhou, X. Xiong, J. Pan, D. Cai, Z. Wei, X. Chen, Y. Liu, N. Luo, J. Yan, T. Fujita, Doping strategy on improving the overall cathodic performance of double perovskite $\text{LnBaCo}_2\text{O}_{5+\delta}$ (Ln = Pr, Gd) as potential SOFC cathode materials, *J. Materiomics.* 9 (2023) 825–837. <https://doi.org/10.1016/j.jmat.2023.02.004>.
- [26] K.E. Song, J.W. Lee, Y.R. Lim, S.W. Baek, T.H. Shin, S. Lee, H. Schlegel, J.H. Kim, Influence of microstructure and applied current on the electrical conductivity of $\text{SmBaCo}_2\text{O}_{5+\delta}$ cathode in solid oxide fuel cell, *Int. J. Hydrogen Energy.* 47 (2022) 15875–15886. <https://doi.org/10.1016/j.ijhydene.2022.03.056>.

- [27] A. Egger, E. Bucher, M. Yang, W. Sitte, Comparison of oxygen exchange kinetics of the IT-SOFC cathode materials $\text{La}_{0.5}\text{Sr}_{0.5}\text{CoO}_{3-\delta}$ and $\text{La}_{0.6}\text{Sr}_{0.4}\text{CoO}_{3-\delta}$, *Solid State Ionics*. 225 (2012) 55–60. <https://doi.org/10.1016/j.ssi.2012.02.050>.
- [28] B. Wei, Z. Lü, X. Huang, M. Liu, N. Li, W. Su, Synthesis, electrical and electrochemical properties of $\text{Ba}_{0.5}\text{Sr}_{0.5}\text{Zn}_{0.2}\text{Fe}_{0.8}\text{O}_{3-\delta}$ perovskite oxide for IT-SOFC cathode, *J. Power Sources*. 176 (2008) 1–8. <https://doi.org/10.1016/j.jpowsour.2007.09.120>.
- [29] A. Mineshige, M. Kobune, S. Fujii, Z. Ogumi, M. Inaba, T. Yao, K. Kikuchi, A. Mineshige, et al., Metal–Insulator Transition and Crystal Structure of $\text{La}_{1-x}\text{Sr}_x\text{CoO}_3$ as Functions of Sr-Content, Temperature, and Oxygen Partial Pressure, *J. Solid State Chem.* 142 (1999) 374–381. <https://doi.org/10.1006/jssc.1998.8051>.
- [30] C. Sun, R. Hui, J. Roller, Cathode materials for solid oxide fuel cells: a review, *J. Solid State Electrochem.* 14 (2010) 1125–1144. <https://doi.org/10.1007/s10008-009-0932-0>

Figure captions

Figure 1. X-ray diffraction (XRD) results of different compositions of the SBSCF 2.05 oxide system.

Figure 2. Electrical conductivity as a function of Fe substitution at 0.1 A.

Figure 3. Electrical conductivity measured with applied current measured at 600 °C under (a) air during the temperature heating process, (b) air during the temperature cooling process, (c) N₂ during the temperature heating process, and (d) N₂ during the temperature cooling process.

Figure 4. Electrical conductivity measured under alternating high oxygen partial pressure (air atmosphere) and low oxygen partial pressure (nitrogen atmosphere) for (a) SBSCF 2.05-0, (b) SBSCF 2.05-0.3, (c) SBSCF 2.05-0.5, and (d) SBSCF 2.05-0.7.

Table captions

Table 1. Abbreviations used in the SBSCF 2.05 oxide system.

Table 2. Electrical conductivity measurement conditions.

Table 3. Electrical conductivity values measured with applied current at 600 °C.

Table 4. Electrical conductivity values as a function of oxygen partial pressure changes (under an applied current of 0.1 A and 300 °C).

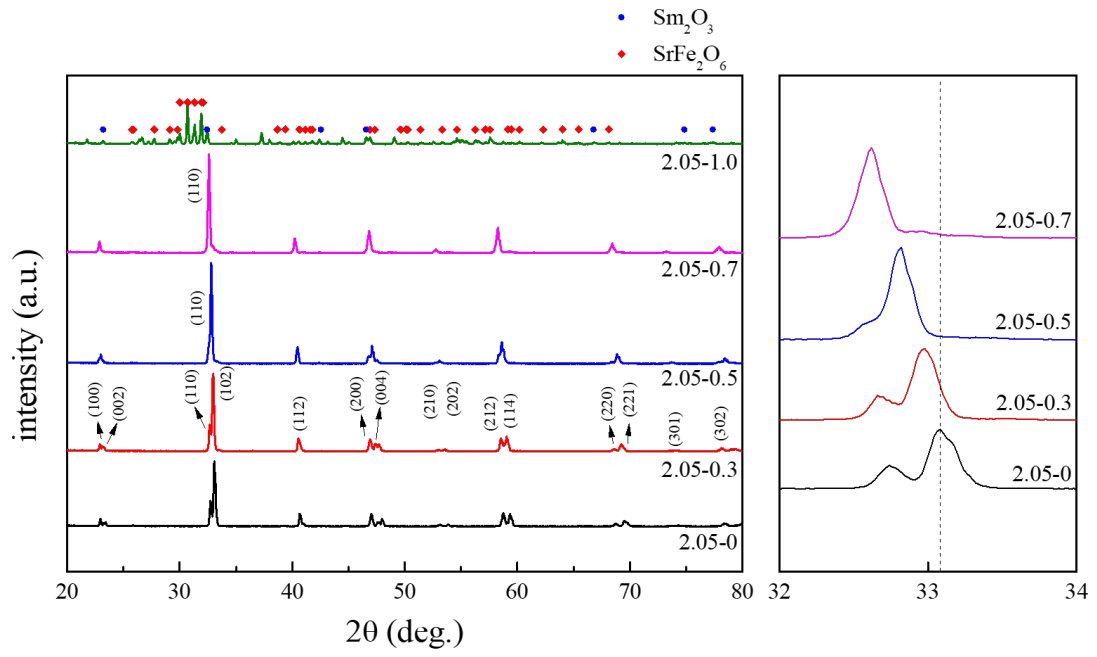


Fig 1. X-ray diffraction (XRD) results of different compositions of the SBSCF 2.05 oxide system.

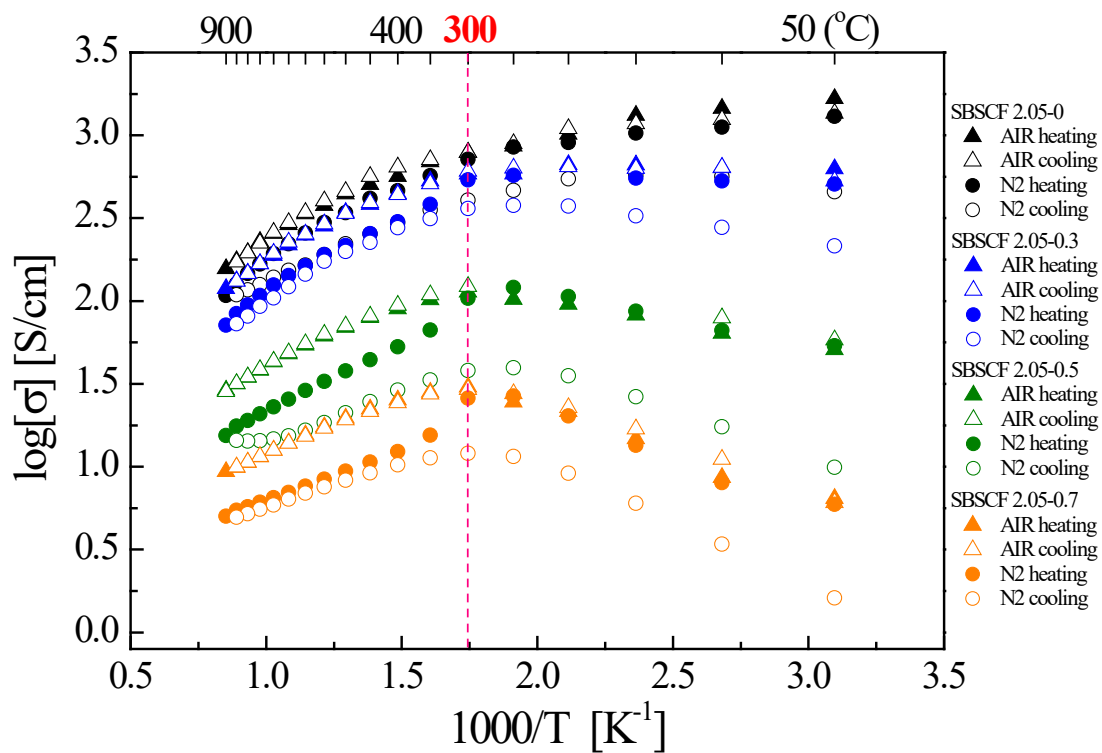
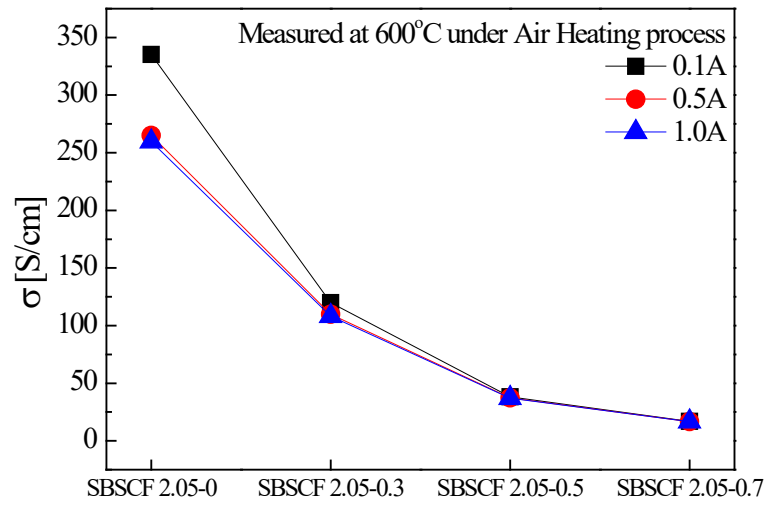
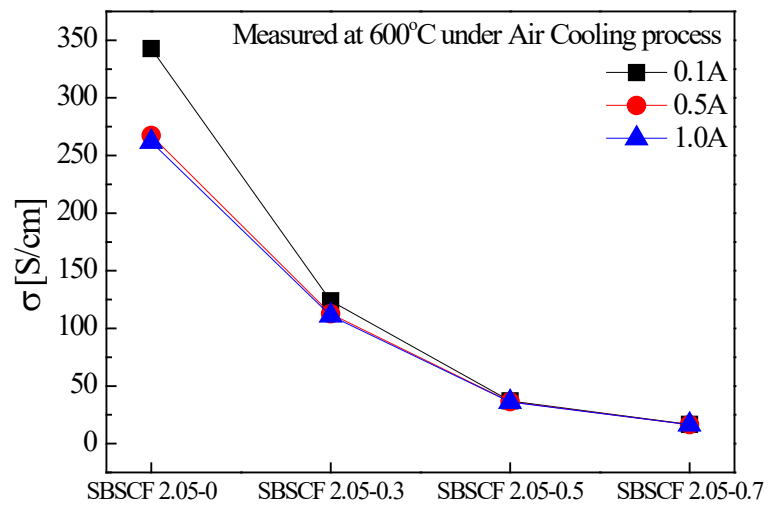


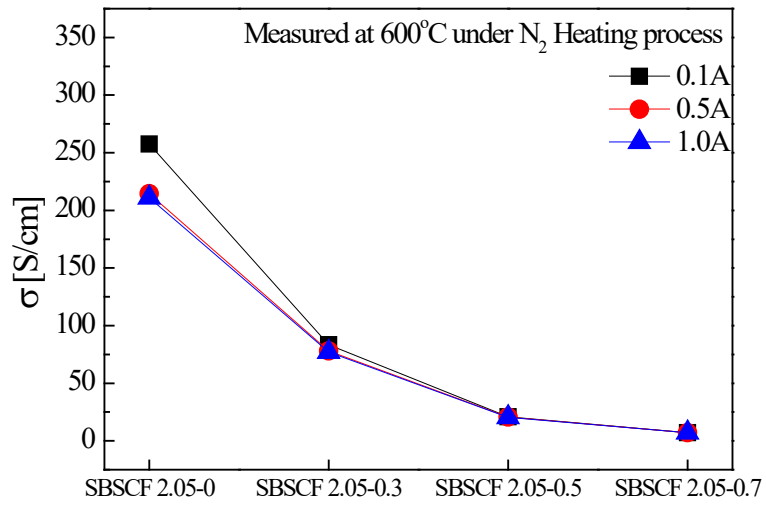
Fig 2. Electrical conductivity as a function of Fe substitution at 0.1 A.



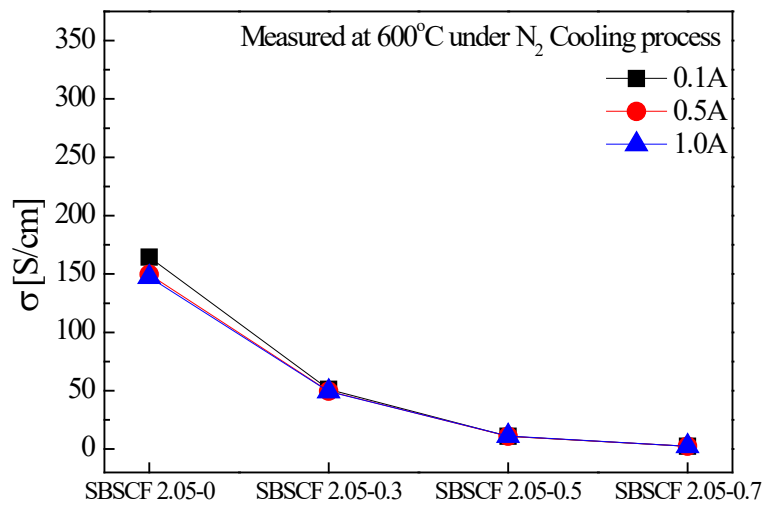
(a)



(b)

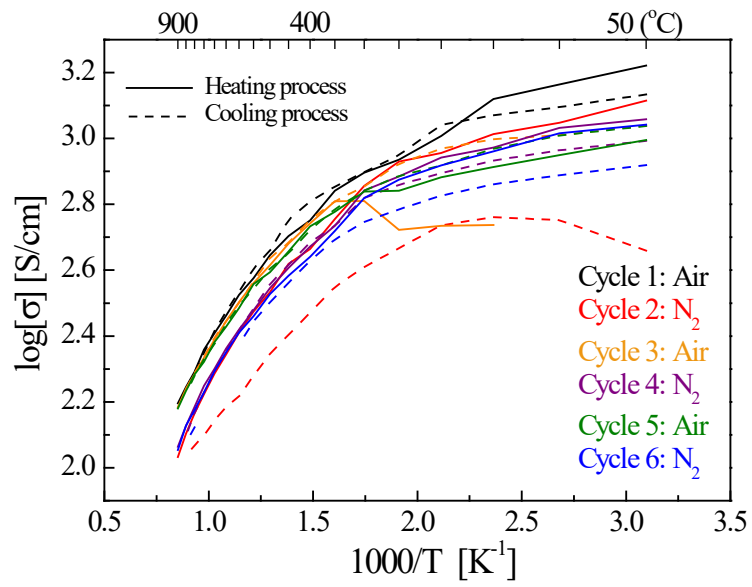


(c)

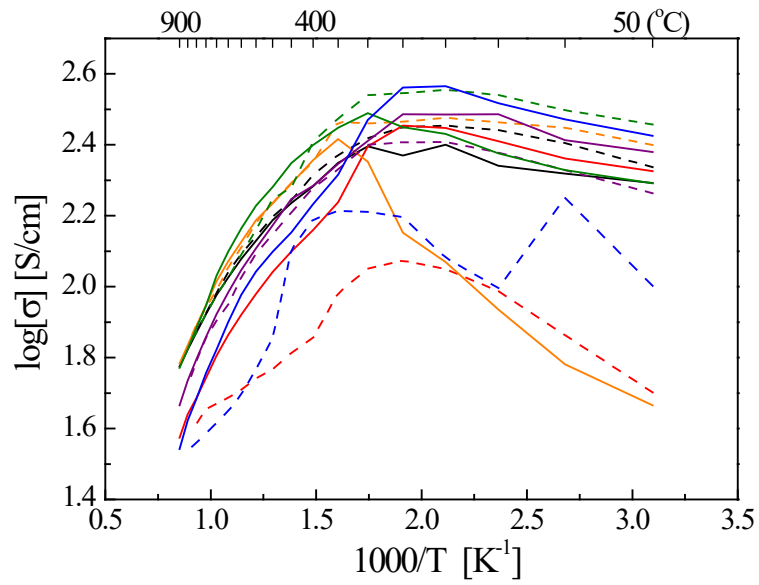


(d)

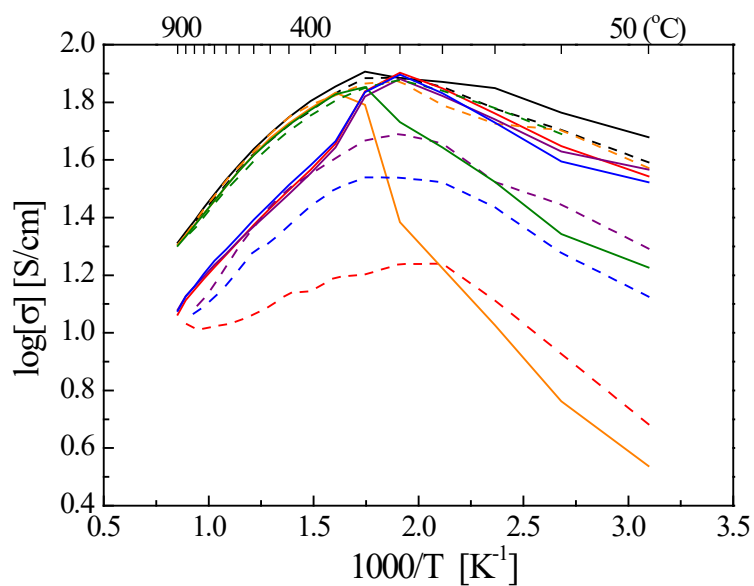
Fig 3. Electrical conductivity measured with applied current measured at 600 °C under (a) air during the temperature heating process, (b) air during the temperature cooling process, (c) N₂ during the temperature heating process, and (d) N₂ during the temperature cooling process.



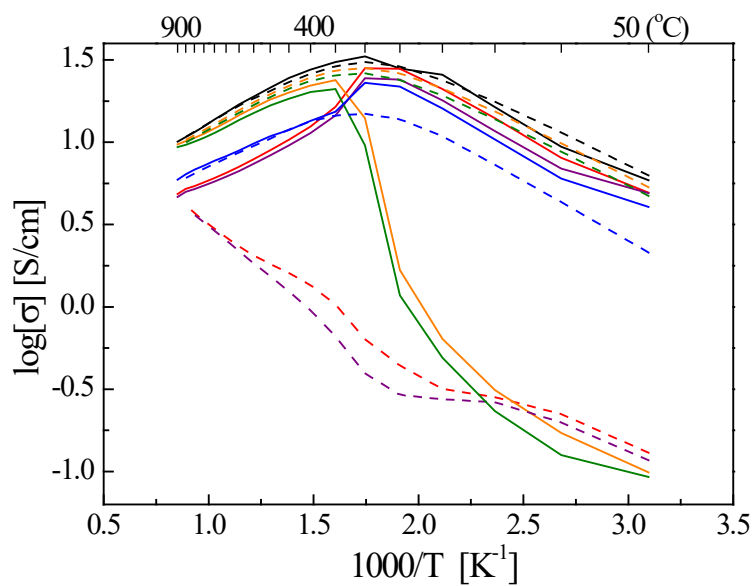
(a)



(b)



(c)



(d)

Fig 4. Electrical conductivity measured under alternating high oxygen partial pressure (air atmosphere) and low oxygen partial pressure (nitrogen atmosphere) for (a) SBSCF 2.05-0, (b) SBSCF 2.05-0.3, (c) SBSCF 2.05-0.5, and (d) SBSCF 2.05-0.7.

Table 1. Abbreviations used in SBSCF 2.05 oxide system.

x	Composition	Abbreviation
0	$\text{SmBa}_{0.5}\text{Sr}_{0.48}\text{Co}_{2.05}\text{O}_{5+d}$	SBSCF 2.05-0
0.3	$\text{SmBa}_{0.5}\text{Sr}_{0.48}(\text{Co}_{0.7}\text{Fe}_{0.3})_{2.05}\text{O}_{5+d}$	SBSCF 2.05-0.3
0.5	$\text{SmBa}_{0.5}\text{Sr}_{0.48}(\text{Co}_{0.5}\text{Fe}_{0.5})_{2.05}\text{O}_{5+d}$	SBSCF 2.05-0.5
0.7	$\text{SmBa}_{0.5}\text{Sr}_{0.48}(\text{Co}_{0.3}\text{Fe}_{0.7})_{2.05}\text{O}_{5+d}$	SBSCF 2.05-0.7
1.0	$\text{SmBa}_{0.5}\text{Sr}_{0.48}\text{Fe}_{2.05}\text{O}_{5+d}$	SBSCF 2.05-1.0

Table 2. Electrical conductivity measurement conditions.

Cycle	Atmosphere	Applied current (A)	Temperature (°C)
Cycle 1			
Cycle 3	Air atmosphere	0.1/ 0.5/ 1.0	Heating process (50 °C ~900 °C) / Cooling process (900 °C ~ 50 °C)
Cycle 5			
Cycle 2	Nitrogen atmosphere		
Cycle 4			
Cycle 6			

Table 3. Electrical conductivity values measured with applied current at 600 °C.

SBSCF 2.05-0	0.35A2	0.65A0	2.59A5
SBSCF 2.05-0.3	119.8	109.7	108.1
SBSCF 2.05-0.5	38.3	37.3	37.1
SBSCF 2.05-0.7	17.0	16.6	16.6

Table 4. Electrical conductivity values as a function of oxygen partial pressure changes (under an applied current of 0.1 A and 300 °C).

	SBSCF 2.05-0		SBSE 2.05-0.3		SBSCF 2.05-0.5		SBSCF 2.05-0.7	
	Up	Down	Up	Down	Up	Down	Up	Down
Cycle 1	787.4	790.3	248.8	262.0	38.4	37.5	8.0	9.9
Cycle 2	717.2	406.6	248.6	112.6	32.4	21.6	6.3	6.5
Cycle 3	646.3	714.7	225.0	191.4	30.4	35.2	8.8	9.4
Cycle 4	694.8	658.8	257.8	251.2	32.7	22.5	6.7	5.5
Cycle 5	689.6	694.3	308.3	346.9	28.7	33.2	7.9	9.4
Cycle 6	659.3	557.7	295.4	162.4	30.3	27.9	6.1	5.5